

**Controllable unidirectional magnetoresistance in ferromagnetic films with broken symmetry**Shun Wang,<sup>1</sup> Xiaotian Cui<sup>1</sup>,<sup>✉</sup> Ronghuan Xie,<sup>1</sup> Changwen Zhang,<sup>1</sup> Yufeng Tian,<sup>2</sup> Lihui Bai,<sup>2</sup>  
Qikun Huang,<sup>1,2,\*</sup> Qiang Cao,<sup>1,†</sup> and Shishen Yan<sup>1,2,‡</sup><sup>1</sup>*Spintronics Institute, University of Jinan, Jinan 250022, China*<sup>2</sup>*School of Physics, State Key Laboratory of Crystal Materials, Shandong University, Jinan 250100, China*

(Received 15 December 2022; revised 21 February 2023; accepted 28 February 2023; published 13 March 2023)

Spin-related unidirectional magnetoresistance (UMR) exhibits nonreciprocal transport to either charge current or magnetization reversal, providing a potential application for direct electrical readout of in-plane magnetization using simple two-terminal geometry. To achieve such a UMR, it is usually believed that an adjacent heavy metal or other materials with strong spin-orbit coupling (SOC) as the spin polarizer is indispensable, leading to most efforts on multilayer structures rather than single-layer ferromagnetic films. Here, we report the observation of UMR in a single CoPt film by introducing a vertical composition gradient to break the structural inversion symmetry. Moreover, unlike conventional heavy-metal/ferromagnetic-metal bilayer films, the UMR in the CoPt film with a positive Co composition gradient is controllable as a function of current amplitude, which shows the decrease, sign reversal, and then enhancement with the increment of current density. These results reveal two competing UMR mechanisms with opposite signs in electrical current dependency, i.e., bulk Rashba effect induced by composition gradients and anomalous Nernst effect driven by a vertical temperature gradient. Our work provides a promising way to manipulate the UMR in a single ferromagnetic film with the combination of charge-spin conversion and magnetothermal effect.

DOI: [10.1103/PhysRevB.107.094410](https://doi.org/10.1103/PhysRevB.107.094410)**I. INTRODUCTION**

The inversion symmetry breaking in nanomagnetic systems plays an important role in the interplay of charge transport and magnetization [1–9]. Among a wide variety of phenomena related to inversion symmetry breaking, nonreciprocal unidirectional magnetoresistance (UMR) has received a great deal of research attention over the past few years due to both fundamental and practical implications [10–17]. In contrast to twofold symmetric magnetoresistance (MR) effects, such as anisotropic magnetoresistance (AMR) [18], spin Hall magnetoresistance (SMR) [19–21], Rashba-Edelstein magnetoresistance [22,23], and Hanle magnetoresistance [24–26], spin-related UMR exhibits an asymmetric resistance response to 180° magnetization reversal, which is of potential to identify the in-plane magnetization orientation without utilizing complex giant magnetoresistance (GMR) or tunnel magnetoresistance structures [27,28]. In fact, the UMR has been demonstrated for the electrical reading of multilevel resistance states which are used to realize magnetic multibit-per-cell memory devices in a two-terminal spin valve stack [29]. So far, the UMR was mainly reported in a bilayer composed of strong spin-orbit coupled (SOC) material and magnet, such as heavy-metal (HM)/ferromagnetic-metal (FM) bilayers [10,30], topological insulator (TI)/FM heterostructures [13,31], HM/TI [32], HM/ferromagnetic insulators [15], and

TI/ferromagnetic semiconductors [33], where HMs and TIs materials as the spin polarizer generate a spin current or net nonequilibrium spin density via spin Hall (SHE) and/or the Rashba-Edelstein effect (REE). These experiments all involve multilayer structures, and the UMR arises mainly from the modulation of the interface resistance through spin-dependent scattering. Recent studies have shown that the contribution of interfacial scattering to the UMR generally has the same sign and prevails in the limit of thin FM, independent of the magnitude of the magnetic field and current [12], which hinders the modulation of the UMR sign in multifunctional devices. From an application point of view, it is of great interest to achieve a bulk UMR in FM film only, as this would allow further simplification of the device structure and may offer the possibility to manipulate the sign of UMR. However, the research of UMR in a common FM film is very rare since most frequently used FM films such as Fe, Co, Ni, FeCo, FePt, and CoPt cannot generate a net spin current density or spin current due to their centrosymmetric structure [34,35].

In our previous works, the bulk spin-orbit torque (SOT) with no need for an extra heavy-metal layer was realized to switch the magnetization of CoPt alloy films via a vertical composition gradient to break the inversion symmetry [36,37]. The inversion asymmetry together with spin-orbit coupling leads to charge-to-spin conversion through the bulk Rashba effect; one may wonder if the CoPt composition gradient films can serve as an excellent platform to investigate the UMR in a single FM film. Here, three types of CoPt gradient films were fabricated, namely, CoPt films with positive Co composition gradient, CoPt films with negative Co composition gradient, and normal CoPt films without composition

\*qkuang@sdu.edu.cn

†qiangcao@126.com

‡shishenyan@sdu.edu.cn

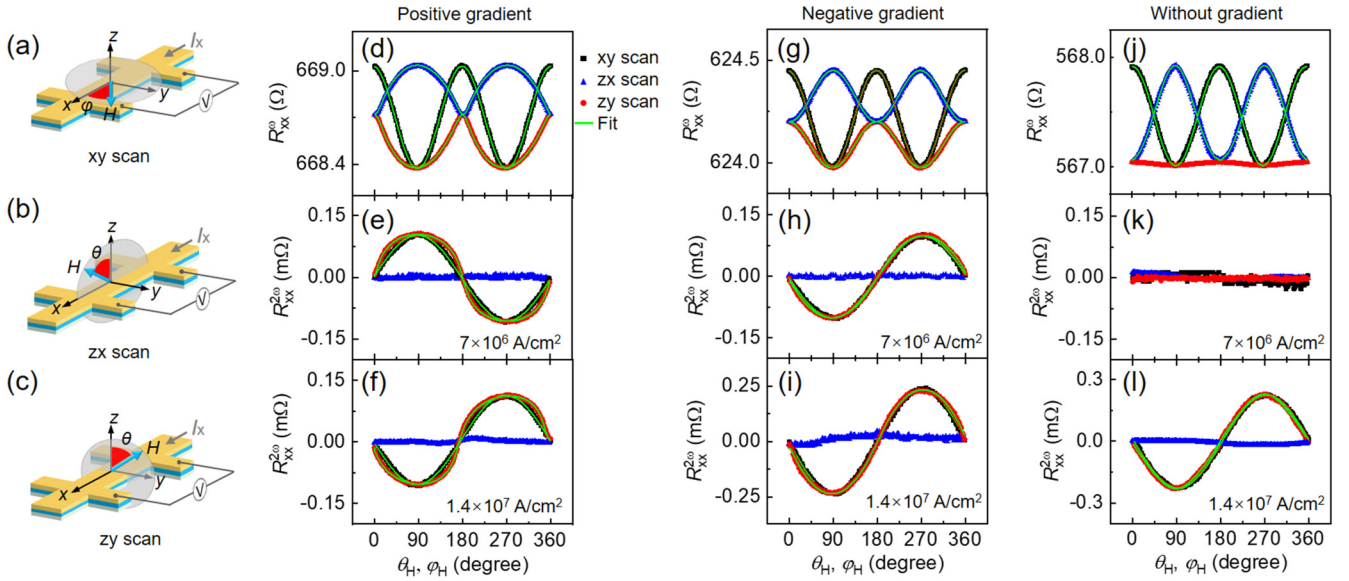


FIG. 1. Angle-dependent longitudinal harmonic resistance of three types of CoPt films with different composition gradients. (a)–(c) Geometric schematic of the measurement and definitions of rotation planes. External magnetic field  $H$  is set to 9 kOe. First-harmonic resistance  $R_{xx}^{1\omega}$  measured at  $J_x = 7 \times 10^6$  A/cm $^2$  for CoPt films with positive (d), negative (g), and without (j) Co composition gradients. A SMR-like behavior is observed in CoPt films with positive and negative Co composition gradients. Second-harmonic resistance  $R_{xx}^{2\omega}$  measured at  $J_x = 7 \times 10^6$  A/cm $^2$  for CoPt films with positive (e), negative (h), and without (k) Co composition gradients. Positive and negative Co composition gradients result in the opposite UMR. Second-harmonic resistance  $R_{xx}^{2\omega}$  measured at a high current density of  $J_x = 1.4 \times 10^7$  A/cm $^2$  for CoPt films with positive (f), negative (i), and without (l) Co composition gradients. In this case, all samples show the same negative UMR. The green solid lines represent the fit to the raw data.

gradient, respectively, corresponding to the positive, negative, and negligible spin Hall angle ( $\theta_{SH}$ ). Therefore, our samples are allowed to adjust the direction of the spin polarization of spin current and thus the sign of UMR by changing the vertical component gradient. Experimental results show that the positive (negative) Co composition gradient leads to a positive (negative) UMR at low current densities. As the current increases, anomalous Nernst effect (ANE) driven by a vertical temperature gradient is gradually dominated, resulting in all CoPt films exhibiting the same negative UMR. As a result, we can observe a controllable UMR in CoPt films with a positive Co composition gradient due to the combination of spin accumulation and magnetothermal effect.

## II. PREPARATION OF SAMPLES AND MEASUREMENT METHODS

Three types of CoPt alloys with different composition gradients are prepared on thermally oxidized Si(001)/SiO $_2$  substrates by magnetron sputtering, i.e., Pt(0.7)/Co(0.1)/Pt(0.3)/Co(0.3)/Pt(0.1)/Co(0.7) (noted as CoPt films with positive Co composition gradient), Co(0.7)/Pt(0.1)/Co(0.3)/Pt(0.3)Co(0.1)/Pt(0.7) (CoPt films with negative Co composition gradient), and normal Pt(0.5)/Co(0.5)/Pt(0.5)/Co(0.5)/Pt(0.5)/Co(0.5) (CoPt films without composition gradient). The numbers in parentheses represent thickness in nanometers. A 2-nm Ru buffer layer is used to improve the crystal quality, and a 2-nm MgO capping layer was grown to prevent CoPt oxidation in the atmosphere. The Ru, Co, and Pt metal layers were deposited by dc magnetron sputtering with 3-mTorr Ar, and the MgO layer was deposited by rf

sputtered with 6-mTorr Ar. All samples exhibit in-plane magnetic anisotropy and a close saturation magnetization of 1000 emu/cm $^3$  [38]. The above nominal Pt/Co stack eventually forms a CoPt alloy single layer due to atomic diffusion during sputter deposition, which has been confirmed in our previous works by high-angle annular dark-field images and elemental mapping [36,37]. To perform the transport measurements, all samples were patterned into the Hall bar devices with width of 5  $\mu$ m and voltage contacts of 14  $\mu$ m by standard optical lithography and Ar-ion beam etching. The harmonic voltage measurements as a function of angle and temperature are performed in a Quantum Design Physical Property Measurement System with a horizontal rotator probe, in which an ac current of  $I = I_0 \sin(\omega t)$  of amplitude  $I_0$  and frequency  $\omega/2\pi = 1317$  Hz is provided by Keithley 6221 and the first and second-harmonic voltages are recorded simultaneously by lock-in amplifiers (Stanford SR830).

## III. UMR MEASUREMENTS AND INTERPRETATION

As shown in Figs. 1(a)–1(c), the longitudinal first ( $R_{xx}^{\omega}$ ) and second ( $R_{xx}^{2\omega}$ ) harmonic resistances are recorded simultaneously between the contacts by applying an ac current along the current channel (x axis) of the Hall bar while rotating a uniform magnetic field of 9 kOe within the  $xy$ ,  $zx$ , and  $zy$  planes. The direction of the magnetic field is defined by the polar coordinates  $\theta$  and the azimuthal angle  $\varphi$ . Here,  $R_{xx}^{\omega}$  represents the conventional resistances independent of the current direction and magnitude, whereas  $R_{xx}^{2\omega}$  includes those current-dependent nonlinear contributions to resistive,

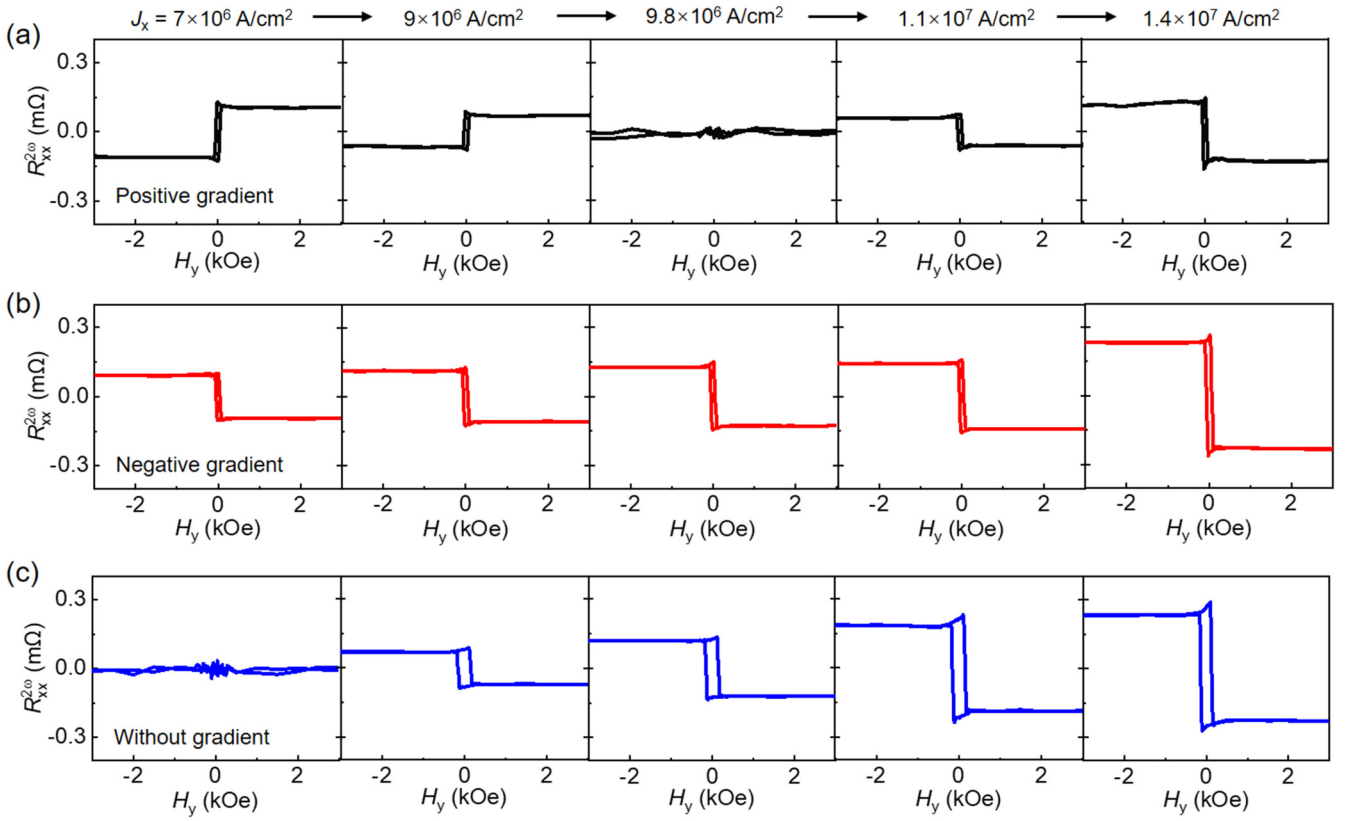


FIG. 2. UMR hysteresis curves  $R_{xx}^{2\omega} - H_y$  as a function of current density. As the current density increases from  $7 \times 10^6$  to  $1.4 \times 10^7$  A/cm<sup>2</sup>, the UMR of CoPt films with positive Co composition gradient changes from positive to negative (a), the UMR of CoPt films with negative Co composition gradient remains negative and increases (b), and the UMR of CoPt films without composition gradient is initially absent and gradually becomes negative (c).

that is the UMR we focus on here. Figures 1(d), 1(g), and 1(j) show the  $R_{xx}^{\omega}$  results for three types of CoPt films, where a typical SMR-like behavior is observed in both CoPt films with positive and negative Co composition gradients, i.e., a sizable MR is present in all three planes and the MR in the  $zy$  plane follows  $-\sin^2 \theta_{zy}$  function. Note that  $\theta_{zy}$  represents the angle of magnetization in the  $zy$  plane, which is slightly deviated from the direction of the external magnetic field due to the in-plane magnetic anisotropy and can be estimated by anomalous Hall resistance [38]. Notably, CoPt films without composition gradient only exhibit the conventional AMR in the  $xy$  and  $zx$  planes as shown in Fig. 1(j), following  $\sin^2 \varphi_{xy}$ , and  $\sin^2 \theta_{zx}$  functions, respectively. Therefore, the SMR-like behavior observed in Figs. 1(d) and 1(g) is related to the composition gradient inside the CoPt films and can be explained as follows: when magnetization  $\mathbf{m}$  of CoPt films is aligned with the spin polarization  $\boldsymbol{\sigma}$  of spin current induced by the bulk Rashba effect, the spin current is less absorbed and converted back to a charge current by the inverse bulk Rashba effect, leading to a decrease in the resistance. If  $\mathbf{m}$  is not collinear with  $\boldsymbol{\sigma}$ , the component of  $\boldsymbol{\sigma}$  perpendicular to  $\mathbf{m}$  will be absorbed and thus increase the resistance.

Figures 1(e), 1(h), and 1(k) show the representative results for  $R_{xx}^{2\omega}$  measured at a low current density of  $7 \times 10^6$  A/cm<sup>2</sup>. We can see that the  $R_{xx}^{2\omega}$  signal is reversed in positive and negative Co gradient films and absent in the films without component gradient. Here, we define a positive UMR

when  $M_y$  is along the  $+y$  direction (i.e.,  $\varphi_{xy}$  and  $\theta_{zy}$  are  $90^\circ$ ) resulting in a high-resistance state ( $R_{xx}^{2\omega} > 0$ ). Thus, the positive (negative) Co composition gradient results in the positive (negative) UMR. The fitted results show that  $R_{xx}^{2\omega} \sim \sin \varphi_{xy} \sin \theta_{zy} \sim \theta_{SH} M_y$ , in agreement with previous reports on UMR in Pt/Co and Ta/Co films with opposite  $\theta_{SH}$  [10]. Therefore, we achieve the UMR in a single CoPt film by introducing a vertical composition gradient and the sign of UMR reverses as the composition gradient changes from positive to negative. More interestingly, we find that all types of CoPt films exhibit the same negative UMR when the current density is increased to  $1.4 \times 10^7$  A/cm<sup>2</sup>, as shown in Figs. 1(f), 1(i), and 1(l), suggesting that the UMR in CoPt films with a positive Co composition gradient can be tuned by current density [Figs. 1(e) and 1(f)], which is different from the fixed-sign UMR in Pt/Co bilayer films [38].

To provide more details on the UMR tuned by current density, we measured the  $R_{xx}^{2\omega} - H_y$  hysteresis curves as a function of current density for three types of CoPt films. As shown in Fig. 2(a), the UMR of CoPt films with a positive Co composition gradient is positive at a low current density of  $J_x = 7 \times 10^6$  A/cm<sup>2</sup>. As the current density increases, the UMR decreases to zero at  $J_x = 9.8 \times 10^6$  A/cm<sup>2</sup> and becomes negative at higher current density. Both the magnitude and the sign of the UMR can be controlled as a function of current density. Note that the critical current density of the UMR reversal can be effectively tuned by changing the thickness of

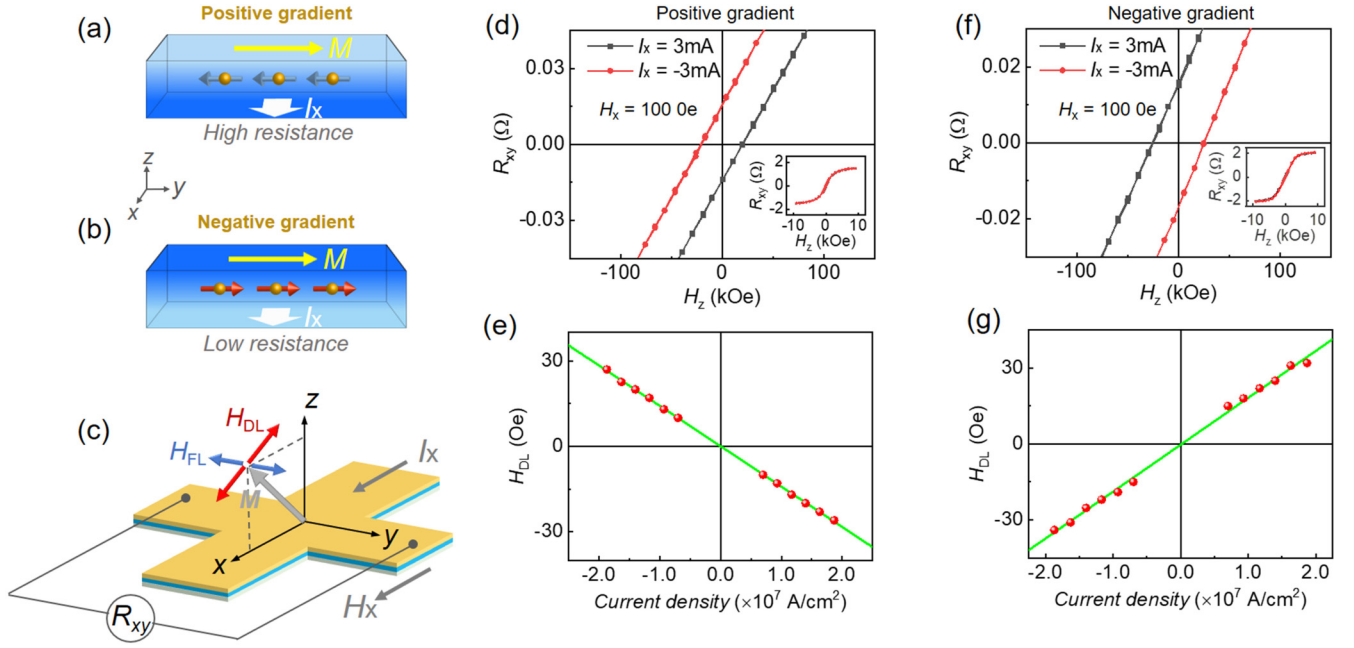


FIG. 3. Bulk Rashba unidirectional magnetoresistance. Illustration of bulk Rashba-induced UMR in the case of positive (a) and negative (b) Co component gradients. (c) Schematics of current-induced SOT effective fields. Magnetization is restricted to rotation in the  $X$  plane in the presence of an in-plane magnetic field  $H_x$ , which gives rise to an out-of-plane component of dampinglike effective field  $H_{DL}$ . Enlarged anomalous Hall resistance loops measured at  $I_x = \pm 3$  mA and a fixed magnetic field  $H_x = 100$  Oe for CoPt films with positive (d) and negative (f) Co component gradients. Insets show the whole loop. Summarized dampinglike effective field  $H_{DL}$  as a function of current densities for CoPt films with positive (e) and negative (g) Co component gradients. Solid lines are a linear fit to the data.

the layer [38]. In contrast, the UMR always remains negative and increases with increasing current density for CoPt films with a negative Co composition gradient [Fig. 2(b)]. For CoPt films without Co composition gradient, as shown in Fig. 2(c), UMR is absent when  $J_x \leq 7 \times 10^6$  A/cm<sup>2</sup> and gradually becomes negative with increasing current density, which is also consistent with the results in Figs. 1(k) and 1(l).

The results suggest that there are two competing mechanisms with opposite signs in electrical current dependency in CoPt films with a positive Co composition gradient. At low current densities, the bulk Rashba effect induced by composition gradients (positive and negative) is responsible for the observed UMR. Nevertheless, an additional negative contribution tends to dominate at high current densities, which depends only on the magnetization direction.

Indeed, the bulk inversion asymmetry in materials along the growth direction ( $z$  axis) leads to a Rashba-type SOC in the form of  $\hat{H}_R = (\alpha_R/\hbar)(z \times \mathbf{P}) \cdot \boldsymbol{\sigma}$  for a conducting electron with momentum  $\mathbf{P}$  [39–41], where  $\alpha_R$  is Rashba parameter,  $\hbar$  is the reduced Planck's constant,  $z$  is a unit vector parallel to the built-in electric field  $\mathbf{E}_z$  given by the bulk symmetry broken,  $\boldsymbol{\sigma}$  is the electron's spin, respectively. As a result of this interaction, the electrons flowing along the  $x$  axis ( $\mathbf{P} // x$ ) experience an effective magnetic field  $\mathbf{H}_R \sim z \times x$  along the  $y$  axis, called the Rashba field, thereby producing a net spin polarization in this direction. Here, for the CoPt films with positive and negative Co composition gradients, the Rashba fields are opposite due to the reverse  $\mathbf{E}_z$ , thus resulting in the opposite spin polarization [38]. In other words, the two samples have opposite  $\theta_{SH}$ . In our previous work [37], we have shown that  $\mathbf{E}_z$  is along the  $+z(-z)$  direction for CoPt films

with a positive (negative) composition gradient. With it, the opposite UMR that appears at low current densities can be explained as illustrated in Figs. 3(a) and 3(b): When an in-plane charge current  $I_x$  is applied along the  $+x$  direction (electrons flowing in the  $-x$  direction), CoPt films with a positive (negative) Co composition gradient produce a spin current with spin polarization  $\boldsymbol{\sigma} // -y(+y)$ . Assuming that the magnetization  $\mathbf{M}$  is saturated along the  $+y$  direction, spin-dependent electron scattering occurring in CoPt films will result in two different resistance states: Giant magnetoresistance (GMR) effect [42–44], i.e., high (low) resistance state for positive (negative) Co composition gradient. Besides, it is worth mentioning that SOT-induced oscillations of magnetization cannot explain the UMR behavior because SOT is minimum when magnetization is aligned with the  $y$  axis ( $\mathbf{m} // \boldsymbol{\sigma}$ ), where  $|R_{xx}^{2\omega}|$  is maximum.

The spin polarization  $\boldsymbol{\sigma}$  of spin current (i.e.,  $\theta_{SH}$ ) induced by the bulk Rashba effect is opposite for positive and negative Co gradients films, which is demonstrated by anomalous Hall resistance  $R_{xy}-H_z$  curves with a constant in-plane magnetic field  $H_x$ . As shown in Fig. 3(c), the dampinglike effective field  $\mathbf{H}_{DL} \sim \boldsymbol{\sigma} \times \mathbf{m}$  has an out-of-plane component when the magnetization  $\mathbf{m}$  is rotating in the  $zx$  plane, thus resulting in a shift of the  $R_{xy}-H_z$  loop along the  $H_z$  axis. Figures 3(d) and 3(f) show the  $R_{xy}-H_z$  loops measured at  $I_x = \pm 3$  mA and  $H_x = 100$  Oe for these two types of composition gradients, where the  $H_z$  value at  $R_{xy} = 0$  represents the current-induced  $H_{DL}$ . We can see that for the same  $I_x$  and  $H_x$ , the  $H_{DL}$  is opposite for positive Co composition gradient and negative Co composition gradient. We further summarize the dependence of  $H_{DL}$  as a function of applied current density in Figs. 3(e) and 3(g), which show that the slope of  $H_{DL}/J_x$  reverses once

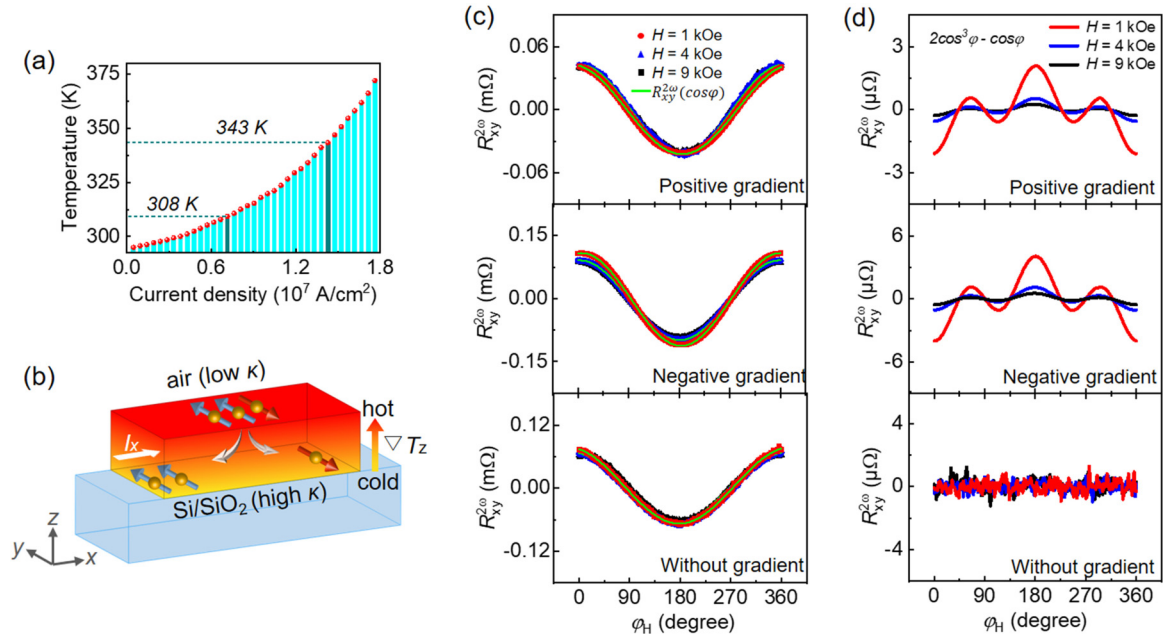


FIG. 4. Contribution of anomalous Nernst effect to unidirectional magnetoresistance. (a) Evaluated temperature of CoPt films with positive Co component gradient as a function of current density. As colored by dark cyan, the temperature is about 308 K at  $J_x = 7 \times 10^6$  A/cm<sup>2</sup> and 343 K at  $J_x = 1.4 \times 10^7$  A/cm<sup>2</sup>. (b) Schematic of current-induced anomalous Nernst effect due to the vertical thermal gradient  $\nabla T_z$ . (c) Measured transverse second-harmonic resistance  $R_{xy}^{2\omega}$  for three types of component gradients. (d)  $H_{FL}$  contribution ( $2\cos^3 \varphi - \cos \varphi$ ) subtracted from the raw data of  $R_{xy}^{2\omega}$  in (c).

the composition gradient is reversed, in agreement with the expectation of opposite spin polarization  $\sigma$  for two types of composition gradients. The spin Hall angle  $\theta_{SH}$  is evaluated as  $\sim 0.079$  ( $-0.096$ ) for the CoPt films with positive (negative) Co composition gradient through  $\theta_{SH} = -2eM_s t_F H_{DL} / \hbar j_e$  [45], which is comparable to that of bulk Pt [46,47]. Here,  $e > 0$  is the electron charge,  $M_s$  is the saturation magnetization,  $t_F$  is the ferromagnetic thickness, and  $j_e$  is the charge-current density.

As discussed in Figs. 1 and 2, the negative UMR mechanism that dominates at high current densities is only related to the magnetization direction and independent of the composition gradient (or bulk Rashba effect). Very recently, it is reported that the normal metal adjacent to FM can induce a nonlinear MR effect by spin AHE, the so-called spin anomalous-Hall UMR [16]. However, we find that the UMR is still observed in SiO<sub>2</sub>/CoPt/MgO structure without the Ru layer [38]. Therefore, the spin anomalous-Hall UMR cannot explain our results here. Next, we show that the ANE associated with the vertical temperature gradient  $\nabla T_z$  is responsible for the observed negative UMR at high current densities. By measuring  $R_{xx}^\omega$  dependence of temperature and current density, we evaluated the temperature of CoPt films as a function of current density [38]. Here, we focus on the results of CoPt films with a positive Co composition gradient. As shown in Fig. 4(a), the temperature of CoPt films is about 308 K at  $J_x = 7 \times 10^6$  A/cm<sup>2</sup> and increases rapidly to 343 K at  $J_x = 1.4 \times 10^7$  A/cm<sup>2</sup> due to current-induced Joule heating. Considering the large difference in thermal conductivity between the SiO<sub>2</sub> substrate ( $\kappa = 1.4$  W m<sup>-1</sup> K<sup>-1</sup>) and air ( $\kappa = 0.024$  W m<sup>-1</sup> K<sup>-1</sup>) [48], the heat dissipation is mainly carried out through the substrate, resulting in a positive  $\nabla T_z$

in CoPt films, as shown in Fig. 4(b). Analogous to the AHE, a transversal spin-polarized charge-current flow in the top and bottom in CoPt films leads to a longitudinal second-harmonic resistance  $R_{xx}^{2\omega}$  as follows:

$$R_{xx}^{2\omega} \propto -\nabla T_z \sin \varphi_{xy} \sin \varphi_{zy}, \quad (1)$$

which fits well the  $R_{xx}^{2\omega}$  results in Figs. 1(f), 1(i), and 1(l). In addition, we note that the vertical temperature gradient also contributes to a spin Seebeck effect (SSE) and thus produces a similar longitudinal UMR by inverse Rashba effect [49]. Unlike ANE, the SSE depends on the conversion from spin currents to charge voltage through the inverse SHE and/or REE. In other words, for two CoPt films with positive and negative Co composition gradients, if SSE dominates, they would have opposite signs due to the opposite  $\theta_{SH}$ . However, as shown in Fig. 2, the UMR always keeps the same (negative) sign at high current densities. For metallic conducting systems, it has been shown that the SSE is less than ANE due to the low ratio of spin currents to charge currents ( $\theta_{SH} \ll 1$ ) [50–52]. Therefore, here SSE is expected to be smaller than ANE.

To experimentally prove the presence of ANE, we investigated the angular dependence of transversal second-harmonic  $R_{xy}^{2\omega}$  during the magnetic field rotation in the  $xy$  plane, which can be described by

$$R_{xy}^{2\omega} = \left( R_{AHE} \frac{H_{DL}}{H} + I_0 \alpha \nabla T_z \right) \cos \varphi + 2R_{PHE} (2\cos^3 \varphi - \cos \varphi) \frac{H_{FL}}{H}, \quad (2)$$

where  $R_{PHE}$ ,  $\alpha$ , and  $H_{FL}$  represent planar Hall resistance, ANE coefficient, and fieldlike effective field (including Oersted

field), respectively. In Eq. (2),  $R_{xy}^{2\omega}$  contains the contributions from  $H_{DL}$ ,  $\nabla T_z$ , and  $H_{FL}$ . However, we note that the contributions of  $H_{DL}$  and  $H_{FL}$  are inversely proportional to the magnetic field while  $\nabla T_z$  is independent of the magnetic field; thus, the contributions of  $H_{DL}$  and  $H_{FL}$  tend to disappear when the magnetic field is large enough to force the magnetization to align strictly along the magnetic field direction, i.e., the  $R_{xy}^{2\omega}$  is approximately equal to

$$R_{xy}^{2\omega} \approx I_0 \alpha \nabla T_z \cos \varphi. \quad (3)$$

Figure 4(c) shows the  $R_{xy}^{2\omega}$  results measured at magnetic fields of 1 kOe, 4 kOe, and 9 kOe for three types of CoPt samples at  $J_x = 1.4 \times 10^7$  A/cm<sup>2</sup>. For positive and negative Co composition gradients, as shown in the top and middle panels of Fig. 4(c),  $R_{xy}^{2\omega}$  changes slightly when the magnetic field is increased from 1 kOe to 9 kOe, suggesting that the signal of  $R_{xy}^{2\omega}$  is mainly due to the contribution of ANE in these large magnetic fields. We further separated the  $H_{FL}$  contribution ( $2\cos^3 \varphi - \cos \varphi$ ) by subtracting the  $\cos \varphi$  fitting curves [the solid lines in Fig. 4(c)] from the raw data of  $R_{xy}^{2\omega}$ . As shown in the top and middle panels of Fig. 4(d), the  $H_{FL}$  contribution has a very small magnitude concerning the raw data of  $R_{xy}^{2\omega}$  and approaches fast to zero at magnetic field  $H = 9$  kOe. Therefore, these results unambiguously demonstrate the existence of an ANE in CoPt films at high current densities. For CoPt without composition gradient,  $R_{xy}^{2\omega}$  is almost no change with increasing the applied magnetic field due to negligible contributions from  $H_{DL}$  and  $H_{FL}$  [bottom panels in Figs. 4(c) and 4(d)]. By Eq. (3), we further estimate the temperature gradient  $\nabla T_z \sim 0.5 \times 10^4$ ,  $1.1 \times 10^4$ , and  $0.8 \times 10^4$  K/m at  $J_x = 1.4 \times 10^7$  A/cm<sup>2</sup> for CoPt films with positive, negative, and without composition gradients, respectively. Here we assume that the same ANE coefficient  $\alpha$  is  $\tilde{3} \times 10^{-6}$  V/KT,

which represents the average value of the Pt-based ferromagnetic systems [53,54].

#### IV. CONCLUSION

In summary, we experimentally investigate the UMR in CoPt alloy films by introducing a vertical component gradient to break the inversion symmetry. Owing to the bulk Rashba effect, a positive (negative) UMR is observed in CoPt films with a positive (negative) Co composition gradient under low current density. As the current increases, the ANE driven by the vertical temperature gradient begins to dominate, giving rise to a negative UMR in all films. As a result, the UMR magnitude shows a continuous process of decrease, sign reversal, and then enhancement in CoPt films with a positive Co composition gradient, which indicates that the UMR is controllable in an electric manner. This work also suggests that composition gradient is a potent way to introduce bulk Rashba SOC in a single ferromagnetic film, which will display more unexpected magnetic properties derived from the strong correlation between spin and momentum.

#### ACKNOWLEDGMENTS

This work was supported by the National Natural Science Foundation of China (Grants No. 11974145 and No. 51871112), the Major Basic Research Project of Shandong Province Grant No. ZR2020ZD28, the 111 Project No. B13029, Independent Cultivation Program of Innovation Team of Jinan City (Grant No. 2021GXRC043), and Taishan Scholar Program of Shandong Province (Grant No. ts20190939).

- 
- [1] I. M. Miron, G. Gaudin, S. Auffret, B. Rodmacq, A. Schuhl, S. Pizzini, J. Vogel, and P. Gambardella, Current-driven spin torque induced by the Rashba effect in a ferromagnetic metal layer, *Nat. Mater.* **9**, 230 (2010).
- [2] G. Q. Yu, P. Upadhyaya, Y. B. Fan, J. G. Alzate, W. J. Jiang, K. L. Wong, S. Takei, S. A. Bender, L. T. Chang, Y. Jiang, M. Lang, J. S. Tang, Y. Wang, Y. Tserkovnyak, P. K. Amiri, and K. L. Wang, Switching of perpendicular magnetization by spin-orbit torques in the absence of external magnetic fields, *Nat. Nanotechnol.* **9**, 548 (2014).
- [3] L. Liu, C. Zhou, X. Shu, C. Li, T. Zhao, W. Lin, J. Deng, Q. Xie, S. Chen, J. Zhou, R. Guo, H. Wang, J. Yu, S. Shi, P. Yang, S. Pennycook, A. Manchon, and J. Chen, Symmetry-dependent field-free switching of perpendicular magnetization, *Nat. Nanotechnol.* **16**, 277 (2021).
- [4] L. You, O. Lee, D. Bhowmik, D. Labanowski, J. Hong, J. Bokor, and S. Salahuddin, Switching of perpendicularly polarized nanomagnets with spin orbit torque without an external magnetic field by engineering a tilted anisotropy, *Proc. Natl Acad. Sci. USA* **112**, 10310 (2015).
- [5] Q. Zhang, J. Liang, K. Bi, L. Zhao, H. Bai, Q. Cui, H. A. Zhou, H. Bai, H. Feng, W. Song, G. Chai, O. Gladii, H. Schultheiss, T. Zhu, J. Zhang, Y. Peng, H. Yang, and W. Jiang, Quantifying the Dzyaloshinskii-Moriya Interaction Induced by the Bulk Magnetic Asymmetry, *Phys. Rev. Lett.* **128**, 167202 (2022).
- [6] L. Liu, Q. Qin, W. Lin, C. Li, Q. Xie, S. He, X. Shu, C. Zhou, Z. Lim, J. Yu, W. Lu, M. Li, X. Yan, S. J. Pennycook, and J. Chen, Current-induced magnetization switching in all-oxide heterostructures, *Nat. Nanotechnol.* **14**, 939 (2019).
- [7] K.-W. Kim, H.-W. Lee, K.-J. Lee, and M. D. Stiles, Chirality from Interfacial Spin-Orbit Coupling Effects in Magnetic Bilayers, *Phys. Rev. Lett.* **111**, 216601 (2013).
- [8] T. Ideue, K. Hamamoto, S. Koshikawa, M. Ezawa, S. Shimizu, Y. Kaneko, Y. Tokura, N. Nagaosa, and Y. Iwasa, Bulk rectification effect in a polar semiconductor, *Nat. Phys.* **13**, 578 (2017).
- [9] K. Ishizaka, M. S. Bahramy, H. Murakawa, M. Sakano, T. Shimojima, T. Sonobe, K. Koizumi, S. Shin, H. Miyahara, A. Kimura, K. Miyamoto, T. Okuda, H. Namatame, M. Taniguchi, R. Arita, N. Nagaosa, K. Kobayashi, Y. Murakami, R. Kumai, Y. Kaneko, Y. Onose, and Y. Tokura, Giant Rashba-type spin splitting in bulk BiTeI, *Nat. Mater.* **10**, 521 (2011).
- [10] C. O. Avci, K. Garello, A. Ghosh, M. Gabureac, S. F. Alvarado, and P. Gambardella, Unidirectional spin Hall magnetoresistance in ferromagnet/normal metal bilayers, *Nat. Phys.* **11**, 570 (2015).

- [11] K. Yasuda, A. Tsukazaki, R. Yoshimi, K. S. Takahashi, M. Kawasaki, and Y. Tokura, Large Unidirectional Magnetoresistance in a Magnetic Topological Insulator, *Phys. Rev. Lett.* **117**, 127202 (2016).
- [12] C. O. Avci, J. Mendil, G. S. D. Beach, and P. Gambardella, Origins of the Unidirectional Spin Hall Magnetoresistance in Metallic Bilayers, *Phys. Rev. Lett.* **121**, 087207 (2018).
- [13] Y. Lv, J. Kally, D. Zhang, J. S. Lee, M. Jamali, N. Samarth, and J. P. Wang, Unidirectional spin-Hall and Rashba-Edelstein magnetoresistance in topological insulator-ferromagnet layer heterostructures, *Nat. Commun.* **9**, 111 (2018).
- [14] T. Guillet, A. Marty, C. Vergnaud, M. Jamet, C. Zucchetti, G. Isella, Q. Barbedienne, H. Jaffrès, N. Reyren, J. M. George, and A. Fert, Large Rashba unidirectional magnetoresistance in the Fe/Ge(111) interface states, *Phys. Rev. B* **103**, 064411 (2021).
- [15] G. Liu, X. G. Wang, Z. Z. Luan, L. F. Zhou, S. Y. Xia, B. Yang, Y. Z. Tian, G. H. Guo, J. Du, and D. Wu, Magnonic Unidirectional Spin Hall Magnetoresistance in a Heavy-Metal-Ferromagnetic-Insulator Bilayer, *Phys. Rev. Lett.* **127**, 207206 (2021).
- [16] M. Mehraeen and S. S. L. Zhang, Spin anomalous-Hall unidirectional magnetoresistance, *Phys. Rev. B* **105**, 184423 (2022).
- [17] L. Chen, K. Zollner, S. Parzefall, J. Schmitt, M. Kronseder, J. Fabian, D. Weiss, and C. H. Back, Connections between spin-orbit torques and unidirectional magnetoresistance in ferromagnetic-metal-heavy-metal heterostructures, *Phys. Rev. B* **105**, L020406 (2022).
- [18] T. R. McGuire and R. I. Potter, Anisotropic magnetoresistance in ferromagnetic in 3d alloys, *IEEE Trans. Magn.* **11**, 1018 (1975).
- [19] H. Nakayama, M. Althammer, Y. T. Chen, K. Uchida, Y. Kajiwara, D. Kikuchi, T. Ohtani, S. Geprags, M. Opel, S. Takahashi, R. Gross, G. E. Bauer, S. T. Goennenwein, and E. Saitoh, Spin Hall Magnetoresistance Induced by a Nonequilibrium Proximity Effect, *Phys. Rev. Lett.* **110**, 206601 (2013).
- [20] J. Kim, P. Sheng, S. Takahashi, S. Mitani, and M. Hayashi, Spin Hall Magnetoresistance in Metallic Bilayers, *Phys. Rev. Lett.* **116**, 097201 (2016).
- [21] J. Fischer, O. Gomonay, R. Schlitz, K. Ganzhorn, N. Vlietstra, M. Althammer, H. Huebl, M. Opel, R. Gross, S. T. B. Goennenwein, and S. Geprägs, Spin Hall magnetoresistance in antiferromagnet/heavy-metal heterostructures, *Phys. Rev. B* **97**, 014417 (2018).
- [22] H. Nakayama, Y. Kanno, H. An, T. Tashiro, S. Haku, A. Nomura, and K. Ando, Rashba-Edelstein Magnetoresistance in Metallic Heterostructures, *Phys. Rev. Lett.* **117**, 116602 (2016).
- [23] J. B. S. Mendes, S. M. Rezende, and J. Holanda, Rashba-Edelstein magnetoresistance in two-dimensional materials at room temperature, *Phys. Rev. B* **104**, 014408 (2021).
- [24] S. Velez, V. N. Golovach, A. Bedoya-Pinto, M. Isasa, E. Sagasta, M. Abadia, C. Rogero, L. E. Hueso, F. S. Bergeret, and F. Casanova, Hanle Magnetoresistance in Thin Metal Films with Strong Spin-Orbit Coupling, *Phys. Rev. Lett.* **116**, 016603 (2016).
- [25] M. I. Dyakonov, Magnetoresistance Due to Edge Spin Accumulation, *Phys. Rev. Lett.* **99**, 126601 (2007).
- [26] H. Wu, X. Zhang, C. H. Wan, B. S. Tao, L. Huang, W. J. Kong, and X. F. Han, Hanle magnetoresistance: The role of edge spin accumulation and interfacial spin current, *Phys. Rev. B* **94**, 174407 (2016).
- [27] C. Lidig, J. Cramer, L. Weißhoff, T. R. Thomas, T. Kessler, M. Kläui, and M. Jourdan, Unidirectional Spin Hall Magnetoresistance as a Tool for Probing the Interfacial Spin Polarization of Co<sub>2</sub>MnSi, *Phys. Rev. Appl.* **11**, 044039 (2019).
- [28] K. Olejník, V. Novák, J. Wunderlich, and T. Jungwirth, Electrical detection of magnetization reversal without auxiliary magnets, *Phys. Rev. B* **91**, 180402(R) (2015).
- [29] C. O. Avci, M. Mann, A. J. Tan, P. Gambardella, and G. S. D. Beach, A multi-state memory device based on the unidirectional spin Hall magnetoresistance, *Appl. Phys. Lett.* **110**, 203506 (2017).
- [30] S. S. L. Zhang and G. Vignale, Theory of unidirectional spin Hall magnetoresistance in heavy-metal/ferromagnetic-metal bilayers, *Phys. Rev. B* **94**, 140411(R) (2016).
- [31] Y. Fan, Q. Shao, L. Pan, X. Che, Q. He, G. Yin, C. Zheng, G. Yu, T. Nie, M. R. Masir, A. H. MacDonald, and K. L. Wang, Unidirectional magneto-resistance in modulation-doped magnetic topological insulators, *Nano Lett.* **19**, 692 (2019).
- [32] C. Ye, X. Xie, W. Lv, K. Huang, A. J. Yang, S. Jiang, X. Liu, D. Zhu, X. Qiu, M. Tong, T. Zhou, C. H. Hsu, G. Chang, H. Lin, P. Li, K. Yang, Z. Wang, T. Jiang, and X. Renshaw Wang, Nonreciprocal transport in a bilayer of MnBi<sub>2</sub>Te<sub>4</sub> and Pt, *Nano Lett.* **22**, 1366 (2022).
- [33] N. H. Duy Khang and P. N. Hai, Giant unidirectional spin Hall magnetoresistance in topological insulator-ferromagnetic semiconductor heterostructures, *J. Appl. Phys.* **126**, 233903 (2019).
- [34] X. Zhang, Q. Liu, J.-W. Luo, A. J. Freeman, and A. Zunger, Hidden spin polarization in inversion-symmetric bulk crystals, *Nat. Phys.* **10**, 387 (2014).
- [35] J. Železný, Z. Fang, K. Olejník, J. Patchett, F. Gerhard, C. Gould, L. W. Molenkamp, C. Gomez-Olivella, J. Zemen, T. Tichý, T. Jungwirth, and C. Ciccarelli, Unidirectional magnetoresistance and spin-orbit torque in NiMnSb, *Phys. Rev. B* **104**, 054429 (2021).
- [36] X. Xie, X. Zhao, Y. Dong, X. Qu, K. Zheng, X. Han, X. Han, Y. Fan, L. Bai, Y. Chen, Y. Dai, Y. Tian, and S. Yan, Controllable field-free switching of perpendicular magnetization through bulk spin-orbit torque in symmetry-broken ferromagnetic films, *Nat. Commun.* **12**, 2473 (2021).
- [37] Q. Huang, C. Guan, Y. Fan, X. Zhao, X. Han, Y. Dong, X. Xie, T. Zhou, L. Bai, Y. Peng, Y. Tian, and S. Yan, Field-free magnetization switching in a ferromagnetic single layer through multiple inversion asymmetry engineering, *ACS Nano* **16**, 12462 (2022).
- [38] See Supplemental Material at <http://link.aps.org/supplemental/10.1103/PhysRevB.107.094410> for magnetic measurements, magnetization angles, angle-dependent harmonic resistance of Pt/Co and Ta/Co samples, tunable critical current density, UMR of CoPt without the Ru layer, temperature as a function of current density, and Rashba fields, which includes Refs. [10,12,17,55,56].
- [39] A. Manchon, H. C. Koo, J. Nitta, S. M. Frolov, and R. A. Duine, New perspectives for Rashba spin-orbit coupling, *Nat. Mater.* **14**, 871 (2015).
- [40] Y. A. Bychkov and É. I. Rashba, Properties of a 2D electron gas with lifted spectral degeneracy, *JETP Lett.* **39**, 78 (1984).
- [41] C. Ciccarelli, L. Anderson, V. Tshitoyan, A. J. Ferguson, F. Gerhard, C. Gould, L. W. Molenkamp, J. Gayles, J. Železný, L. Šmejkal, Z. Yuan, J. Sinova, F. Freimuth, and T. Jungwirth,

- Room-temperature spin-orbit torque in NiMnSb, *Nat. Phys.* **12**, 855 (2016).
- [42] G. Binasch, P. Grunberg, F. Saurenbach, and W. Zinn, Enhanced magnetoresistance in layered magnetic structures with antiferromagnetic interlayer exchange, *Phys. Rev. B* **39**, 4828(R) (1989).
- [43] M. N. Baibich, J. M. Broto, A. Fert, F. Nguyen Van Dau, F. Petroff, P. Etienne, G. Creuzet, A. Friederich, and J. Chazelas, Giant Magnetoresistance of (001)Fe/(001)Cr Magnetic Superlattices, *Phys. Rev. Lett.* **61**, 2472 (1988).
- [44] R. E. Camley and J. Barnas, Theory of Giant Magnetoresistance Effects in Magnetic Layered Structures with Antiferromagnetic Coupling, *Phys. Rev. Lett.* **63**, 664 (1989).
- [45] A. V. Khvalkovskiy, V. Cros, D. Apalkov, V. Nikitin, M. Krounbi, K. A. Zvezdin, A. Anane, J. Grollier, and A. Fert, Matching domain-wall configuration and spin-orbit torques for efficient domain-wall motion, *Phys. Rev. B* **87**, 020402(R) (2013).
- [46] L. Liu, O. J. Lee, T. J. Gudmundsen, D. C. Ralph, and R. A. Buhrman, Current-Induced Switching of Perpendicularly Magnetized Magnetic Layers Using Spin Torque from the Spin Hall Effect, *Phys. Rev. Lett.* **109**, 096602 (2012).
- [47] S. Łazarski, W. Skowroński, J. Kanak, Ł. Karwacki, S. Ziętek, K. Grochot, T. Stobiecki, and F. Stobiecki, Field-Free Spin-Orbit-Torque Switching in Co/Pt/Co Multilayer with Mixed Magnetic Anisotropies, *Phys. Rev. Appl.* **12**, 014006 (2019).
- [48] C. O. Avci, K. Garello, M. Gabureac, A. Ghosh, A. Fuhrer, S. F. Alvarado, and P. Gambardella, Interplay of spin-orbit torque and thermoelectric effects in ferromagnet/normal-metal bilayers, *Phys. Rev. B* **90**, 224427 (2014).
- [49] K.-i. Uchida, H. Adachi, T. Ota, H. Nakayama, S. Maekawa, and E. Saitoh, Observation of longitudinal spin-Seebeck effect in magnetic insulators, *Appl. Phys. Lett.* **97**, 172505 (2010).
- [50] S. Y. Huang, W. G. Wang, S. F. Lee, J. Kwo, and C. L. Chien, Intrinsic Spin-Dependent Thermal Transport, *Phys. Rev. Lett.* **107**, 216604 (2011).
- [51] A. D. Avery, M. R. Pufall, and B. L. Zink, Observation of the Planar Nernst Effect in Permalloy and Nickel Thin Films with In-Plane Thermal Gradients, *Phys. Rev. Lett.* **109**, 196602 (2012).
- [52] M. Schmid, S. Srichandan, D. Meier, T. Kuschel, J. M. Schmalhorst, M. Vogel, G. Reiss, C. Strunk, and C. H. Back, Transverse Spin Seebeck Effect versus Anomalous and Planar Nernst Effects in Permalloy Thin Films, *Phys. Rev. Lett.* **111**, 187201 (2013).
- [53] K. D. Lee, D. J. Kim, H. Yeon Lee, S. H. Kim, J. H. Lee, K. M. Lee, J. R. Jeong, K. S. Lee, H. S. Song, J. W. Sohn, S. C. Shin, and B. G. Park, Thermoelectric signal enhancement by reconciling the spin Seebeck and anomalous Nernst effects in ferromagnet/non-magnet multilayers, *Sci. Rep.* **5**, 10249 (2015).
- [54] T. Seki, Y. Sakuraba, K. Masuda, A. Miura, M. Tsujikawa, K. Uchida, T. Kubota, Y. Miura, M. Shirai, and K. Takahashi, Enhancement of the anomalous Nernst effect in Ni/Pt superlattices, *Phys. Rev. B* **103**, L020402 (2021).
- [55] E. C. Stoner and E. P. Wohlfarth, A mechanism of magnetic hysteresis in heterogeneous alloys, *IEEE Trans. Magn.* **27**, 3475 (1947).
- [56] M. Hayashi, J. Kim, M. Yamanouchi, and H. Ohno, Quantitative characterization of the spin-orbit torque using harmonic Hall voltage measurements, *Phys. Rev. B* **89**, 144425 (2014).